Botulinum neurotoxin: unique folding of enzyme domain of the most-poisonous poison

Raj Kumar [a] , Roshan V. Kukreja [a] , Li Li [a] , Artem Zhmurov [c] , Olga Kononova [c] , Shuowei Cai [a] , Syed A. Ahmed [b] , Valeri Barsegov [c] & Bal Ram Singh [a]

[a] Department of Chemistry and Biochemistry , Botulinum Research Center, University of Massachusetts , Dartmouth , MA , 02747 , USA

[b] Department of Cell Biology and Biochemistry , US Army Medical Research Institute of Infectious Diseases , Ft. Detrick , MD , 21702 , USA

[c] Department of Chemistry , University of Massachusetts , 1 University Ave., Lowell , MA , 01854 , USA

Published online: 08 Jun 2013.

PLEASE SCROLL DOWN FOR ARTICLE

Taylor & Francis
Taylor & Francis Group

Botulinum neurotoxin: unique folding of enzyme domain of the most-poisonous poison

Raj Kumar[a], Roshan V. Kukreja[a], Li Li[a], Artem Zhmurov[c], Olga Kononova[c], Shuowei Cai[a], Syed A. Ahmed[b], Valeri Barsegov[c]* and Bal Ram Singh[a]*

[a]*Department of Chemistry and Biochemistry, Botulinum Research Center, University of Massachusetts, Dartmouth, MA 02747, USA;* [b]*Department of Cell Biology and Biochemistry, US Army Medical Research Institute of Infectious Diseases, Ft. Detrick, MD 21702, USA;* [c]*Department of Chemistry, University of Massachusetts, 1 University Ave., Lowell, MA 01854, USA*

Communicated by Ramaswamy H. Sarma

Botulinum neurotoxin (BoNT), the most toxic substance known to mankind, is the first example of the fully active molten globule state. To understand its folding mechanism, we performed urea denaturation experiments and theoretical modeling using BoNT serotype A (BoNT/A). We found that the extent of BoNT/A denaturation from the native state (N) shows a nonmonotonic dependence on urea concentration indicating a unique multistep denaturation process, $N \rightarrow I_1 \rightleftharpoons I_2 \rightleftharpoons U$, with two intermediate states I_1 and I_2. BoNT/A loses almost all its secondary structure in 3.75 M urea (I_1), yet it displays a native-like secondary structure in 5 M urea (I_2). This agrees with the results of theoretical modeling, which helped to determine the molecular basis of unique behavior of BoNT/A in solution. Except for I_2, all the states revert back to full enzymatic activity for SNAP-25 including the unfolded state U stable in 7 M urea. Our results stress the importance of structural flexibility in the toxin's mechanism of survival and action, an unmatched evolutionary trait from billion-year-old bacteria, which also correlates with the long-lasting enzymatic activity of BoNT inside neuronal cells. BoNT/A provides a rich model to explore protein folding in relation to functional activity.

Keywords: botulinum neurotoxin; protein folding; MD simulations; urea denaturation

Introduction

Botulinum neurotoxin (BoNT) is one of the most toxic proteins known to humankind and is a Class-A biothreat agent. BoNT has been used as an effective therapeutic drug against numerous neuromuscular disorders and for cosmetic purposes corresponding to about two billion dollar industry globally (Katona, 2012; Singh, 2009). The physiological basis underlying the BoNT's-dreaded pathogenicity and therapeutic utility is its long lasting paralytic effects on muscles. Biochemically, this effect is caused by the extraordinary survival of the enzymatic domain of the toxin inside neuronal cells for up to an year (Adler, Keller, Sheridan, & Deshpande, 2001; Dolly & Aoki, 2006; Pickett & Perrow, 2011; Stephan & Wang, 2011). Despite the critical biological importance, the molecular basis of the long intracellular survival of BoNT is not understood. The unusual persistence of BoNT intoxication could be due to any of the following factors: (a) the intracellular stability of the toxin, (b) the long lifetime of the truncated soluble NSF attachment protein receptor (SNARE) fragments, and (c) the intra-cellular modifications of the toxin. While sequence homology among different serotypes of BoNT is rather low (<50%), the sequence homology among the light chains is lower compared with the heavy chains. Hence, the light chains are likely to hold a key to understand the specificity of these proteins.

Each of the seven serotypes of BoNT (A–G) is a 150 kDa protein, which consists of a 100 kDa heavy chain (residues 448–1296) and a 50 kDa light chain (residues 1–448) linked together by a disulfide bond (Cai & Singh, 2001a). A simplified schematic of BoNT serotype A (BoNT/A) is presented in Figure 1(A). Upon selective binding to the pre-synaptic nerves through HC, the toxin is internalized through endocytosis. Consequently, the BoNT LC is delivered into the cytosol where it blocks acetylcholine release at the nerve – muscle junctions (8). The biochemical step in blocking the neurotransmitter release involves the Zn^{2+}-endopeptidase activity of different BoNT LCs against a select group of neuronal proteins (SNAREs), which are critical for the exocytosis of the neurotransmitter (Li & Singh, 2000; Montecucco

---

*Corresponding author. Email: Valeri_Barsegov@uml.edu (V. Barsegov); bsingh@umassd.edu (B.R. Singh)
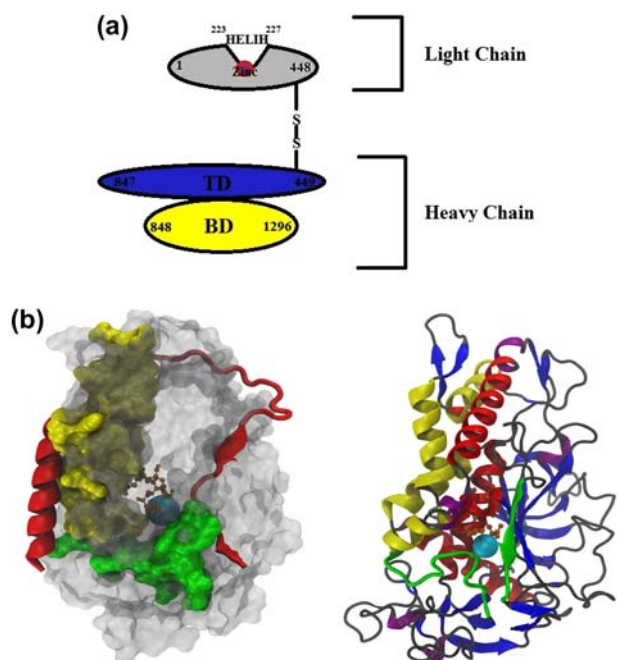
Figure 1.   Panel A: schematic representation of the different domains of botulinum neurotoxin serotype A (BoNT/A) showing the heavy chain (HC) and the light chain (LC) connected by the disulfide bond and the cleavage site. The heavy chain is divided into the binding domain (BD) and the translocation domain (TD). Panel B, *Left*: structural representation of the BoNT/A light chain (BoNT/A LC) showing solvent-accessible surface area (shown in gray color) co-complexed with SNAP-25 peptide (shown in red). The binding interface (groove) is in dark gray color. Also shown are the α-exosite (shown in yellow), β-exosite (shown in green), and the catalytic domain (shown in brown) with the coordinated zinc-ion (blue ball). Panel B, *Right*: cartoon representation of BoNT/A LC showing elements of the secondary structure (color denotation for the α-exosite, β-exosite, and catalytic domain is same as in the left panel): α-helices (shown in orange color), β-sheets (shown in blue), 3_{10}-helices (shown in purple), and random coil and turns (shown in gray).

& Schiavo, 1993). Only entire substrate proteins or their large polypeptide segments are recognized to include exosites for cleavage by BoNT endopeptidases (Breidenbach & Brunger, 2004). All the BoNT endopeptidases exclusively recognize one or more (in case of BoNT/C1) of the three SNARE proteins (syntaxin, SNAP-25, and synaptobrevin) involved in the exocytosis.

The light chain of BoNT (BoNT LC) is a compact globular protein. The most-resolved crystal structure of BoNT/A LC co-complexed with the SNARE substrate (Figure 1(B)) has been reported by Breidenbach and Brunger (Protein Data Bank (PDB) entry: 1XTG; Breidenbach & Brunger, 2004). The secondary structure of BoNT/A LC is a mixture of α-helices and β-sheets. The central portion of this enzyme is the Zn^{2+} binding motif (HEXXH + E), which is conserved among all BoNT LCs. The active site of BoNTs is a very deep but

narrow groove, whereas in thermolysin active site is formed by a broad but shallow surface. The catalytic zinc ion in the active site is coupled to the imidazole ring of residues His223 and His227 and the carboxyl side-chain of residue Glu262. Four flexible loops, 50/60 loop (residues 54–68), 170 loop (residues 156–174), 370 loop (residues 364–368), and 250 loop (residues 237–258), which form the rim of the active site cleft, participate in substrate binding (Figure 1(B), Segelke, Knapp, Kadkhodaya, Balhorn, & Ruoo, 2004). The SNARE proteins bind to the two binding sites in BoNT/ A LC called the α-exosite and the β-exosite. The α-exosite is the interface at the junction of four α-helices formed by residues 102–113 (α-helix 1), 310–321 (α-helix 2), 335–348 (α-helix 3), and 351–358 (α-helix 4). The β-exosite is situated to residues 242–249 in two distorted strands of the 250 loop of BoNT/A LC.

The molten globule (MG) state of proteins is believed to be an important intermediate conformation for protein folding. Although MG structures for many enzymes are known to be inactive in terms of their enzymatic activity (Ptitsyn, Pain, Semisotnov, Zerovnik, & Razgulyaev, 1990; Tsou, 1995), there are several examples of the enzymes, such as xylanase, dihydrofolate reductase (Lopez, Bañares-Hidalgo, & Estrada, 2011; Uversky et al., 1996; Vamvaca, Vogeli, Kast, Pervushin, & Hilvert, 2004) which retain some enzymatic activity in the MG state. It has been shown in our recent studies and by other groups that the BoNT endopeptidase in the MG state retains full enzymatic activity (Cai & Singh, 2001b; Kukreja, Sharma, & Singh, 2010). Because of this, a family of BoNT enzymes is now regarded as a new class of metalloproteases (Montecucco & Schiavo, 1993; Tonello, Morante, Rossetto, Schiavo, & Montecucco, 1996). To this day, BoNT is the only known to be fully enzymatically active MG protein and present an example of biologically important MG structure (Cai & Singh, 2001a, 2001b; Kukreja et al., 2010; Tonello et al., 1996). Hence, an understanding of the mechanism of regulation of unique BoNT endopeptidase activity at the molecular level might hold a key to discern the comprehensive mechanism of BoNT intracellular survival and action. Although a considerable progress has been achieved in recent years, many questions remain. How longevity of the most poisonous poison is related to its folding and thermodynamic stability? How folding pathways account for the emergence of enzymatically active MG state and optimally active PRIME (pre-imminent MG enzyme) state (Kukreja & Singh, 2005)?

To address these questions, we have explored the folding dynamics of the BoNT endopeptidase using BoNT serotype A Light Chain (BoNT/A LC) as a model system. We have utilized urea denaturation assays and Molecular Dynamics (MD) simulations to unmask the folding mechanism. A highly unusual folding pattern has emerged,

which does not show a typical folding co-operativity but rather, it follows a unique three-step denaturation process with two intermediate states, i.e. $N \rightarrow I_1 \rightarrow I_2 \rightarrow U$. This finding agreed with results from MD simulations which enabled us to resolve the structural underpinning of BoNT in the native state (N), intermediate state (I_1 and I_2), and unfolded state (U). Except for the intermediate state I_2, all the states of BoNT/A retained full enzymatic activity for the substrate SNAP-25, including the unfolded state U stable in 7 M urea solution. Direct observation of the functionally active intermediate states of BoNT defines a unique folding pattern and specifies the crucial role played by partially unfolded intermediate conformations. Our results stress the importance of the structural heterogeneity and conformational flexibility in the toxin's mechanism of intracellular survival and action.

Materials and methods

Unfolding and refolding assays on BoNT/A and BoNT/E light chains

BoNT/A LC was dialyzed against the buffer P (10 mM sodium phosphate, 50 mM NaCl and 1 mM di-thiothreitol, pH = 7.4) and diluted to a fixed concentration of .5 mg/ml in a series of aqueous urea solutions of varying concentrations. All the mixtures were equilibrated for at least 2 h at room temperature (25 °C). To prepare denatured BoNT/A LC stock for refolding assays, urea solution was added to BoNT/A LC solution to a final concentration of 8 M and the sample was incubated for 2 h for complete unfolding. To dilute the denatured BoNT/A LC to various final concentrations of urea, same aliquot of stock BoNT/A LC in 8 M urea was taken and different amounts of buffer P (phosphate buffer) was added. BoNT/A LC molecules were allowed to refold for 15 h at room temperature. Similar method was used for the preparation of urea denatured sample of BoNT/E LC. The concentration of BoNT/E LC was .25 mg/ml.

Monitoring secondary and tertiary structure of BoNT/A light chain

Circular dichroism (CD) spectra were recorded using a Jasco Model 715 at a speed of 20 nm/min with a response time of 8 s and a path length of 1 nm at 25 °C. Thermal denaturation of BoNT/A LC dissolved in buffer containing 0, 1, 2, 3, 3.75, and 7 M urea was followed by monitoring the CD signal at $\lambda = 222$ nm. The temperature-induced unfolding of BoNT/A LC was followed by analyzing the temperature-induced changes in the CD signal at $\lambda = 222$ nm (θ_{222}). Each sample was heated and the ellipticity (θ_{222}) was recorded every .2 °C in 20–70 °C temperature range. In these experiments, temperature was raised at the rate of 1 °C/min. Fluorescence spectra were recorded on a ISS K2 fluorimeter (Champaign, IL) using .1 mg/ml sample of BoNT/A. Protein solutions

were excited at $\lambda = 295$ nm and emission spectra were recorded in 310–400 nm range. The excitation and emission slits were fixed at 4 and 8 nm, respectively.

FTIR-based analysis of secondary structure of BoNT/A light chain

BoNT/A LC was diluted to a fixed concentration of LC (1.2 mg/ml) and was dissolved in 10 mM sodium phosphate buffer (pH = 7.4) containing 50 mM NaCl, 1 mM DTT, and urea at different concentrations. For this assay, we used 0, 3.75, 5, and 7 M concentrations of aqueous urea. Obtained solutions of BoNT/A LC were then incubated at room temperature for 2 h. The Fourier Transform Infrared (FTIR) spectra of BoNT/A LC and BoNT/A LC with 3.75, 5, and 7 M urea were recorded using a Nicolet 4200 FTIR (Nicolet Corp., Madison, WI). The sample compartment is made of a 45 horizontal zinc selenide attenuated total reflectance. The spectra were collected with 512 scans at 4 cm^{-1} resolution, and a 7-point Savitsky – Golay smoothing was applied. The final IR spectra were generated after subtraction of the appropriate reference spectra. Since urea interfered significantly in the amide-I and -II regions, analysis of spectra were performed in the amide-III region (1230–1330 cm^{-1}). All the spectra were analyzed using the Gaussian fit by Thermo Nicolet omnic software (version 6.0) with a constant baseline, FWHH (full width at half height) at 10 and sensitivity at medium.

Enzymatic activity of BoNT/A light chain

The endopeptidase activity of urea-denatured BoNT/A LC was assayed using a full length peptide SNAP-25 and the SNAPtide peptide (FITC/DABCYL; List Biologicals, Campbell, CA) as substrates. The 12-amino acid long peptide SNAPtide is derived from SNAP-25 and contains residues TRIDQANQRATK (Boldt et al., 2006). First, .5 mg/ml protein samples were incubated for 2 h in different urea solutions. After exposure to the denaturing agent, the enzymatic activity was assayed in buffer containing no urea. All the assays were carried out at 37 °C in 100 ml reaction volumes in a 96-well plate. Each well contained 1 μl of protein (100 nM), 2.5 μl SNAPtide (5 mM), and 96.5 μl assay buffer which contained 20 mM HEPES, 1.25 mM DTT, and .1% Tween-20 (pH = 7.4). The untreated BoNT/A LC was used as positive control and each assay was performed for 1 h. The plate was read in SpectraMax M5 microplate reader (Molecular devices, Menlo Park, CA, USA) using the excitation wavelength of 490 nm, emission wavelength of 523 nm, and the cut-off at 495 nm. The endopeptidase activity of BoNT/A was estimated by comparing the fluorescence intensities of the control SNAPtide with that of the cleaved SNAPtide. The endopeptidase activity of urea-denatured BoNT/A LC was also measured with His-tag SNAG (SNAPGFPHIS, batch No.SNAG-His6169SR, MW ∼ 57 kDa), using 100 nM BoNT/A LC and 2 μM

SNAG in 100 μl reaction mixture. Cleavage products were ∼28 and ∼26 kDa on sodium dodecyl sulfate poly-acrylamide gel electrophoresis (SDS-PAGE). Extent of cleavage was monitored by nonreducing SDS-PAGE. Urea-denatured BoNT/A LC was incubated with SNAG in 10 mM sodium phosphate buffer (pH = 7.4) containing 50 mM NaCl and 1 mM DTT for 1 h. The reaction was stopped by the addition of 100 μl SDS loading buffer. 20 μl of each sample was loaded on a lane of the gel along with kaleidoscope marker (Bio-Rad, 161–0375, Hercules, CA). The electrophoresis was run using a Mini Protean II system from Bio-Rad at a constant voltage of 120 V at 25 °C. After electrophoresis, the gels were stained with Coomassie blue stain to visualize protein bands. Densitometric analysis was performed to quantify uncleaved SNAG using Kodak software.

MD simulations of BoNT/A light chain in urea solution

All-atomic modeling of BoNT/A LC was performed using the resolved crystal structure of the truncated portion of BoNT/A LC, which includes the amino acid residues 2–422 (PDB entry: 2ISE). MD simulations were performed in 0, 3.75, 5, and 7 solutions of urea in water using the NAMD 2.7 software package (Phillips et al., 2005) and the CHARMM22 force field (MacKerell et al., 1998). To prepare a model system for each urea concentration, we placed the appropriate number of urea molecules in the solvation box and added the corresponding number of water molecules. Each initial protein structure was solvated with at least 15 Å of TIP3P water (Jorgensen, Chandrasekhar, Madura, Impey, & Klein, 1983). To model 50 mM concentration of NaCl, the appropriate number of counter ions was included to neutralize the net electric charge. The details of preparation of all the model systems are presented in the Supporting Material (SM). In the active site of BoNT/A, Zn^{2+} was covalently linked to residues His223, His227, and Glu262. Next, each model system was energy-minimized using the steepest descent algorithm, and heated to room temperature ($T = 25$ °C), and equilibrated for .5 ns in the NPT ensemble (N is the total number of atoms, P is pressure, and T is temperature). Periodic boundary conditions were applied to all water and urea molecules. The van der Waals interactions were turned off at a 10–12 Å distance, and the nonbonded interactions were truncated at 13.5 Å. The short-range nonbonded interactions and the long-range electrostatic forces were computed at each step. The particle mesh Ewald summation method was used to describe the long-range electrostatics. At the production stage, one long 100 ns MD simulation run was performed for each model systems (Table S1 in SM). Structural analysis of the simulation output was performed using the Visual Molecular Dynamics (VMD) package (Humphrey, Dalke, & Schulten, 1996) and the

in-house software. We analyzed the secondary structure by using the "Timeline" option in the VMD package. We also analyzed the tertiary structure of BoNT/A LC using the distance-dependent structure overlap function, $\xi(t) = 1/2N(N-1)\sum_{i\neq j=1}^{N} \Theta(|r_{ij}(t) - r_{ij}^0| - \beta r_{ij}^0)$. In $\Theta(x)$ (Heaviside step function), in the double summation over the C_α-atoms representing amino acid residues, $r_{ij}(t)$ and r_{ij}^0 are the interparticle distances between the i-th and j-th residues in the transient structure and in the native structure, respectively ($\beta = .2$ is the tolerance for the distance change). Structure overlap function $\xi(t)$ is a suitable measure of the extent of structural similarity between a given conformation and a reference state (native state).

Results

Unfolding of BoNT/A LC and BoNT/E LC in urea

We studied structural changes in BoNT/A LC in aqueous urea using CD spectroscopy (see Methods). We analyzed dynamic secondary structure alterations which accompany unfolding of BoNT/A LC by monitoring the CD signals at $\lambda = 222$ nm (θ_{222}). This is a suitable measure of the α-helicity of a protein. The results from denaturation experiments are presented in Figure 2. We see that, first, θ_{222} gradually decreases when the urea concentration increases to 3.75 M, then increases until the urea concentration reaches 5 M value, and then decreases again (Figure 2(A)). Hence, the BoNT/A LC unfolds, refolds, and re-unfolds, while populating the two partially-unfolded intermediate states, denoted as I_1 and I_2 that are stable in 3.75 M and 5 M urea solution, respectively. Analysis of CD spectra of BoNT/A LC revealed that when populating the first intermediate state (I_1), the molecule loses some of its α-helical structure, whereas in the second intermediate state (I_2), the molecule restores its α-helicity adopting the native-like structure. To determine whether this folding pattern is unique to BoNT/A LC, we have repeated unfolding assays for BoNT serotype E (BoNT/E). The profiles of θ_{222} for BoNT/A LC and BoNT/E LC are compared in Figure 2(B). We see that the curve of θ_{222} for BoNT/E LC shows a typical S-shaped monotonic dependence on the concentration of urea with no detectable intermediate species.

Our observation of two additional transitions for BoNT/A LC, $N \rightarrow I_1 \rightarrow I_2 \rightarrow U$ from the native state (N) to the globally unfolded state (U), i.e. transitions $N \rightarrow I_1$ and $I_1 \rightarrow I_2$, is unique indeed. The first intermediate state I_1 loses its secondary structure whereas the second intermediate state I_2 maintains its secondary structure as indicted, respectively, by a low and high CD signal for these states (Figure 2 and the inset). We have arrived at same conclusions analyzing the FTIR spectra (data not shown). The features of FTIR spectra
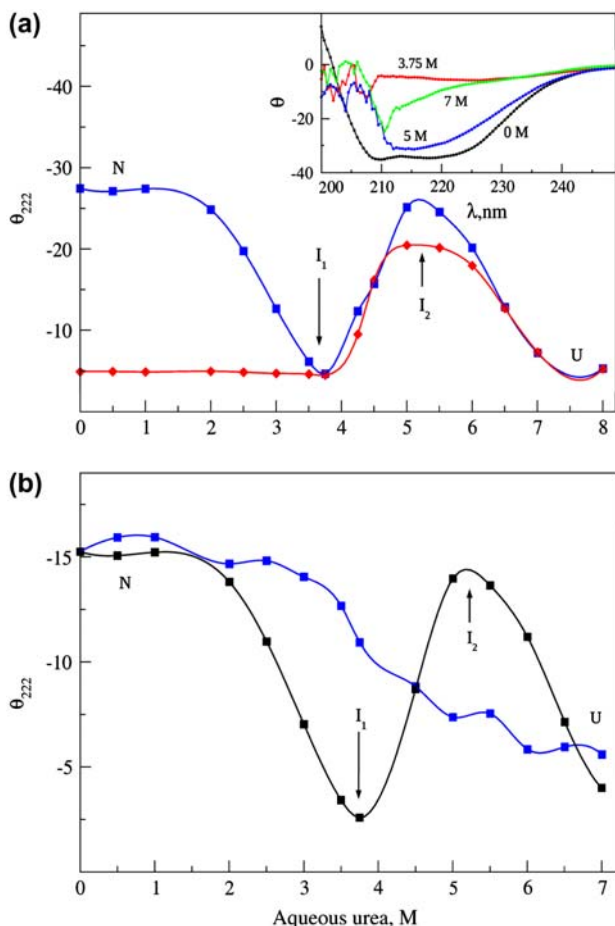
Figure 2. Unfolding of BoNT/A endopetidase domain in urea solution. Panel A: urea-induced denaturation (blue squares connected by the blue curve) and renaturation (red diamonds connected by the red curve) of BoNT/A LC (.5 mg/ml) at room temperature ($T = 25\,°C$) monitored by far UV-CD signal at $\lambda = 222\,nm$, θ_{222} (see Methods). θ_{222}, which quantifies the amount of α-helical content of BoNT/A LC undergoing unfolding from the native state (N) to the globally unfolded state (U), exhibits the nonmonotonic dependence on the urea concentration. The minimum and maximum of the denaturation curve (blue curve), observed in 3–6 M range of urea concentration signifies the formation of stable intermediate states (denoted as I_1 and I_2). The inset shows far UV/CD spectra of BoNT/A LC in 200–250 nm range, which correspond to the different concentrations of urea solution. Panel B: comparison of denaturation curves monitored by far UV-CD signal θ_{222} at room temperature, for BoNT/A LC (.2 mg/ml) and BoNT/E LC (.2 mg/ml). The monotonic dependence of θ_{222} on urea concentration for BoNT/E LC shows that the three-step unfolding mechanism is unique for BoNT/A.

summarized in Table 1 have confirmed our finding, namely, that upon the first transition ($N \rightarrow I_1$), there is a significant increase in the share of random coil up to 57.7% (state I_1) from 34.5% (native state N). In the second transition ($I_1 \rightarrow I_2$), the combined share of α-helices and β-sheets increases to 59.3%, which is comparable to

Table 1. Summary of the secondary structure content of BoNT/A LC (α-helices, β–sheets, and random coil and turns) for different values of urea concentration. The propensities for each secondary structure element given by the percentage and standard deviations, are derived from the FTIR curve fitting (see Methods).

Secondary structure	BoNT/A LC in 0 M urea (%)	BoNT/A LC in 3.75 M urea (%)	BoNT/A LC in 5 M urea (%)	BoNT/A LC in 7 M urea (%)
α-helices	$33.9 \pm .5$	24.0 ± 1.2	$16.7 \pm .3$	10.2 ± 3.4
β-sheets	31.6 ± 2.9	18.4 ± 1.1	42.6 ± 1.5	40.1 ± 3.1
Random coil and turns	34.5 ± 2.4	57.7 ± 2.2	40.2 ± 1.9	$49.6 \pm .3$

66.5% for the native state, and a share of random coil decreases to 40.2% (state I_2) from 57.7% (state I_1).

Thermal unfolding of BoNT/A LC

To understand the unique mechanism of BoNT/A LC denaturation, we studied thermal unfolding of urea-denatured BoNT/A LC (see Methods). We monitored CD signal (θ_{222}) to probe dynamic transitions at the secondary structure level. For each value of urea concentration, we profiled θ_{222} as a function of temperature. The obtained curves of θ_{222} displayed in Figure 3 were then used to estimate the melting temperature. The melting temperature (t_m) first decreased from $t_m \approx 48\,°C$ for urea-free solution (native state N) to $t_m \approx 34\,°C$ for 3.75 M urea solution (intermediate state I_1), but then increased to $t_m \approx 50\,°C$ for 5 M urea solution
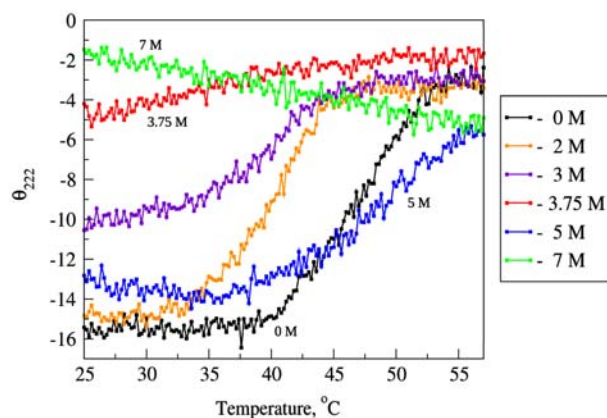
Figure 3. Thermal unfolding of BoNT/A endopetidase domain in aqueous urea as a function of urea concentration. Thermal denaturation curves were generated by dissolving BoNT/A (.25 mg/ml) in buffer P at room temperature ($T = 25\,°C$) and heating the sample at a rate of 1 °C per min. The progress of unfolding was monitored by continuous measurement of the CD signal θ_{222} (see Methods). Thermal denaturation curves are shown for 0, 2, 3, 3.75, 5, and 7 M aqueous solutions of urea (color denotation is presented in the graph).

(intermediate state I_2). Interestingly, the profile of θ_{222} for 5 M urea was similar to that for the native protein (0 M urea), but the transition range was broader (see Figure 3) suggesting a non-cooperative unfolding transition. This is indicative of a highly flexible native structure, which has been implicated in a variety of studies of the functional activity of BoNT/A endopeptidase (Burnett et al., 2005; Kukreja & Singh, 2005). We also found while populating the intermediate conformation I_1 (3.75 M urea) that BoNT/A LC tends to aggregate in a short period of time ($\sim$15 min) even when a moderate .26 mg/ml concentration of protein is used. Next, we repeated this experiment using a ten-fold lower concentration of the protein (.02 mg/ml). At this concentration, it took $\sim$4 h to see aggregation, which resulted in a permanent loss of a CD signal. On contrast, the second intermediate state (I_2), which shows the native-like secondary structure, remained stable and formed a clear solution in 5 M urea.

The initial decrease in t_m for 3.75 M urea-treated BoNT/A LC (I_1 state) was followed by the increase in t_m for 5 M urea solution (I_2 state), which indicates that I_2 has a relatively rigid structure. This was also supported by similar values of enthalpy change for thermal denaturation, i.e. $\Delta H = 297.80 \pm 10.55$ kJ/mol for the native state N vs. $\Delta H = 205.11 \pm 9.83$ kJ/mol for the intermediate state I_2. The thermal denaturation profiles for I_2 was not as sharp as that for the native state N, which indicates a loss of the tertiary structure for BoNT/A LC in state I_2 (Figure 2). These findings are consistent with the data from Trp fluorescence spectroscopy, i.e. $\lambda_{max} = 324$ nm for 0 M urea vs. $\lambda_{max} = 334$ nm for 5 M urea (see next paragraph). Hence, our results imply that in BoNT/A LC, a hydrophobic collapse and formation of the secondary structure occurs simultaneously, a conclusion also corroborated, e.g. by our renaturation data (Figure 2(A), red curve). In view of the high enthalpy cost, the initial collapse is likely due to formation of a network of hydrogen bonds, rather than formation of a hydrophobic core.

We also examined dynamic changes in BoNT/A LC at the tertiary structure level by monitoring the Trp-fluorescence signal (see Methods). To suppress the contribution from fluorescence of Tyr residue, we used the excitation wavelength $\lambda = 295$ nm. The profile of the wavelength, which corresponds to the maximum of the fluorescence intensity λ_{max} as a function of urea concentration, is shown in Figure 4. Not surprisingly, the native fold (N) shows $\lambda_{max} \approx 324$ nm, which indicates that Trp residues in BoNT/A LC are in a hydrophobic environment (17). When the urea concentration is increased, λ_{max} shifts to 351 nm (unfolded state U) indicating that upon denaturation, Trp residues become increasingly more exposed to a polar environment (urea molecules). Furthermore, the profile of λ_{max} is not a typical S-shaped curve. Rather, λ_{max} shows a monotonic increase up to
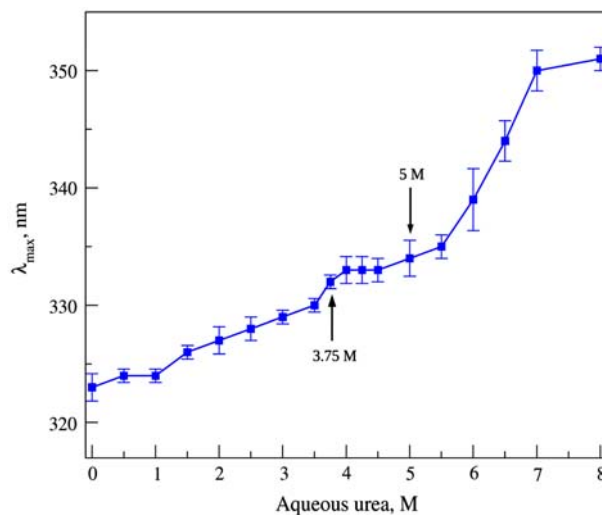

Figure 4. Fluorescence maximum, λ_{max} for BoNT/A LC in aqueous urea solution as a function of urea concentration. To collect the fluorescence data, BoNT/A LC (.1 mg/ml) was dissolved in buffer P at room temperature ($T = 25\,^\circ$C) containing urea. Samples were excited at $\lambda = 295$ nm and the wavelength corresponding to the maximum of fluorescence intensity were recorded for each concentration of urea (see Methods). The profile of λ_{max} shows a small plateau around 3.75–5 M concentration of urea.

3.75 M urea, which is interrupted by the plateau of roughly constant $\lambda_{max} \approx 333$–334 nm in the 3.75–5 M range. Beyond 5 M urea, λ_{max} increases again attaining 351 nm level at 8 M concentration of urea (Figure 4). These distinct regimes of the dependence of λ_{max} on urea concentration reflect the three consecutive unfolding transitions $N \rightarrow I_1 \rightarrow I_2 \rightarrow U$ and confirm our results from urea denaturation experiments and thermal unfolding assays, namely that the intermediate states I_1 and I_2 are stable in 3.75–5 M range (Figures 2 and 3).

Enzymatic activity of BoNT/A LC

To determine whether the intermediate states I_1 and I_2 remained functional, we measured endopeptidase activity of BoNT/A LC in 3, 3.75, 4.5, 5, and 7 M solution of aqueous urea (see Methods). The data on enzyme activity vs. urea concentration are presented in Figure 5, where we have compared the results for the full-length substrate SNAP-25 and the truncated 12-mer SNAPtide (see Methods). In the case of SNAPtide, the first intermediate state I_1 exhibits significant enzymatic activity ($\sim$35%), whereas it is reduced to less than 10% for the second intermediate state I_2. This is somewhat counterintuitive, given that I_2 has native-like secondary structure (Figure 2). Even in 7 M urea solution (unfolded state U), BoNT/A LC shows high enzymatic activity ($\sim$35%) comparable with that of the intermediate state I_1. The results for SNAPtide correlate well with our findings for SNAP-25, albeit enzymatic activity for SNAP-25 was
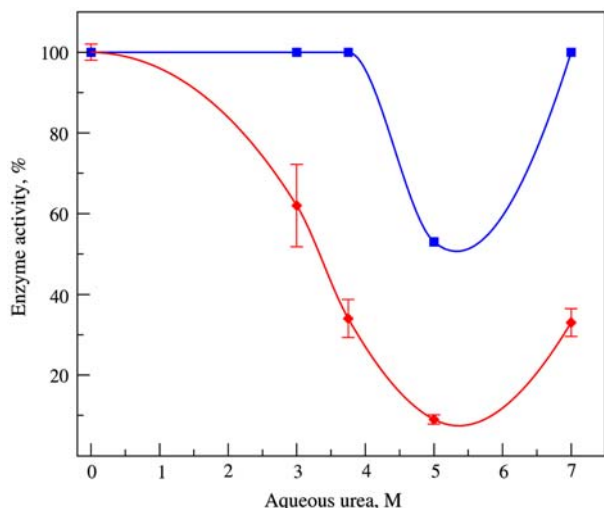
Figure 5. Endopeptidase activity of BoNT/A LC as a function of urea concentration (smooth curves connecting the data points are to guide the eye). 100 nM of BoNT/A LC, initially denatured in urea solution, was reconstituted in a urea-less buffer (100-fold dilution) containing 5 μM of SNAPtide (see Methods) and the assay was carried out at $T = 37\,°C$. The enzymatic activity of BoNT/A in the presence of SNAPtide (red diamonds connected by red curve) is compared with the activity of BoNT/A for SNAP-25 (blue squares connected by blue curve).

uniformly higher as compared to that for SNAPtide. We also found that BoNT/A LC remained fully active in 7 M urea (Figure 5).

In the case of a simple two-state folder, there is dynamic equilibrium between the folded and unfolded states at intermediate urea concentrations. In the case of the four-state model for BoNT/A folding, a more realistic picture would be that the statistical ensemble of protein molecules is as a distribution of several interconverting forms. That is to say that there is dynamic equilibrium between the first and second intermediate states ($I_1 \varsigma I_2$) at intermediate values of urea concentration (3.8–5 M) and between the second intermediate state and the unfolded state ($I_2 \varsigma U$) at high concentration of urea (5–7 M). However, our denaturation experiments show the transition from native state to the first intermediate state at low concentration of urea (1–3.8 M) is irreversible ($N \rightarrow I_1$). Hence, the unique unfolding pattern of BoNT/A LC can be described by the three-step kinetic scheme: $N \rightarrow I_1 \varsigma I_2 \varsigma U$. Consequently, the measured endopeptidase activity of BoNT/A LC in urea solution of higher concentration (> 3.8 M) is a sum of enzyme activities for different protein forms (I_1, I_1, and U).

MD simulations of BoNT/A LC unfolding in aqueous urea

To provide the molecular-level picture underlying the unique mechanism of BoNT/A folding, we carried out

MD simulations of BoNT/A LC in urea-free solution (control), and in 3.75, 5, and 7 solution of aqueous urea at $T = 25\,°C$. For each urea concentration, we performed one long 100 ns simulation run, wherein, we monitored dynamic changes to the secondary and tertiary structures of the enzyme (see Methods). First, we analyzed the propensities to α-helices, β-sheets, and random coil and turns as a function of the simulation time. The last 10 ns portion of the "secondary structure dynamics" per-residue basis for BoNT/A LC is compared in Figure S1 in the Supporting Material (SM). Dynamic changes in the tertiary structure of BoNT/A LC are presented in Figure S2 in SM.

The secondary structure of BoNT/A LC is fairly similar under urea-free solution conditions (0 M urea) and in 5 M urea. In the case of 5 M urea solution, we observed a short 5 Å elongation of the α-helix formed by residues 259–265 and 277–299, and formation of two short α-helices (residues 367–372 and 377–383). By contrast, for BoNT/A LC in 3.75 M and 7 M urea solution, substantial changes in the secondary structure were detected (Figure S1). In 3.75 M urea solution, an interesting change in the secondary structure was observed. Most of the α-helical segments transformed into turns (residues 80–96, 101–112, 216–231, 259–265, 268–272, 277–294, 309–320, 334–342, and 350–357), and 3_{10}- and π-helices (residues 97–99, 223–231, and 295–298). Yet, the β-sheets remained mostly unchanged (residues 18–22, 32–38, 41–47, 134–137, 143–146, 150–154, 163–165, 183–186, 191–197, 210–213, 371–375, and 412–416). Hence, MD simulations provide evidence that in 3.75 M urea solution, BoNT/A LC has the β-sheet structure. Because such structures are prone to self-aggregation, we think that it is the abundance of random-coil which facilitates the formation of aggregates detected in our thermal unfolding assays. In 7 M urea solution, several α-helical segments and β-sheets transformed into random coil, yet random coil in certain parts of the molecule turned into α-helix. Residues 216–232 and 277–299 which formed α-helices and residues 32–38, 41–47, 133–138, 183–186, 191–197, 210–213, 322–324, 330–332, 371–375, and 413–417, which formed β-sheets in 5 M urea solution and formed random coil in 7 M urea solution. Residues 17–22, 146–154, 168–173, 268–272, 356–365, and 394–401 which formed β-sheets and random-coil in 5 M urea solution had become part of the α-helical structure in 7 M urea solution. In addition, the length of the remaining α-helices decreased from 25.5 (residues 216–232) and 34.5 Å (residues 277–299) to 10.5 and 22.5 Å, respectively.

Our results of the tertiary structure analysis showed that BoNT/A LC preserves its tertiary structure under urea-free conditions (folded state U) and 3.75 M urea conditions (first intermediate state I_1; see Figure S2). Indeed, the structure overlap decreases by only a few

percent in 100 ns time interval. In contrast, BoNT/A LC gradually loses 40 and 70% of its tertiary structure in 5 M urea solution (intermediate state I_2) and 7 M urea solution (unfolded state U) within the same time interval. Yet, a large amount of the tertiary structure, i.e. 60% for state I_2 and 30% for state U, is preserved. Hence, the amount of tertiary structure in BoNT/A LC molecule monotonically decreases with the increasing concentration of urea in the following order $N > I_1 > I_2 > U$ (see Figure S1). This tendency BoNT/A LC molecule has to be contrasted with its secondary structure propensity to form α-helices and β-sheets, which exhibits a non-monotonic dependency on the urea concentration (i.e. $N > I_2 > I_1 > U$; Figure S2). The structures of BoNT/A LC obtained at the end of the simulation run for each solution condition are displayed in Figure 6.

The main results from MD simulations are the following: BoNT/A LC was stable in urea-free solution (i.e. no unfolding in the native state N); lost most of its α-helical content but retained almost all β-sheets while preserving the tertiary structure in 3.75 M urea (partial unfolding – first intermediate state I_1); regained some of its α-helical content while preserving most (∼60%) of its tertiary structure in 5 M urea (partial refolding – second

intermediate state I_2); and lost almost all of its α-helices and all β-sheets in 7 M urea (complete denaturation to form the unfolded state U). Comparing the structures of BoNT/A LC in urea-free solution and in 7 M urea solution (Figure 6), we see that the protein molecule has unfolded almost completely, i.e. it lost almost all of its secondary structure elements (only a few α-helices remained intact) and almost all (∼70%) of its tertiary structure. Hence, our simulation results agree with our experimental findings regarding the three-step folding mechanism: $N \rightarrow I_1 \rightarrow I_2 \rightarrow U$. In addition, our simulation results provide information about the structure of the two intermediate states, I_1 and I_2 (Figure 6).

The 100 ns length of our simulation runs is short compared with the typical 10^0–10^1 μs timescales of protein unfolding, which might introduce some inaccuracy in the simulation results. Yet, the dynamics of changes in the secondary structure show systematic changes, rather than fluctuations (Figure S1). Hence, notwithstanding the short length of simulations compared with the expected unfolding timescale and the imperfections of the force field, our MD simulations seem to capture the main experimental findings which validates our approach.

Discussion and conclusion

To understand the dynamic behavior of BoNT molecules in solution, which is an important first step to discern the macroscopic mechanism of extraordinary intracellular survival and action displayed by a family of BoNT molecules, it is necessary to illuminate their folding mechanism at the sub-molecular level and resolve the crucial structural determinants. Unfortunately, this goal cannot be accomplished by analyzing the crystal structure alone, as crystal-packing forces might dictate a particular arrangement of protein molecules in a unit cell. This might lead to substantial differences in their (secondary and tertiary) structure in the crystal state and in the solution. By using a combination of experimental techniques and computer simulations, we have demonstrated, for the first time, a unique folding pattern with two stable intermediate states, i.e. $N \rightarrow I_1 \leftrightharpoons I_2 \leftrightharpoons U$, for the BoNT/A LC serotype A and have described the unfolding mechanism. Both experimental measurements and MD simulations indicate strongly that the secondary structure propensity (α-helices plus β-sheets) changes nonmonotonically with increased concentration of the denaturing agent (urea). We demonstrated an almost complete loss of the secondary structure in the first intermediate state (I_1), an almost full recovery of the secondary structure in the second intermediate state (I_2), and a complete loss of the secondary structure in the globally unfolded state (U). MD simulations indicate a (monotonic) gradual loss of the tertiary structure in the order $N > I_1 > I_2 > U$.
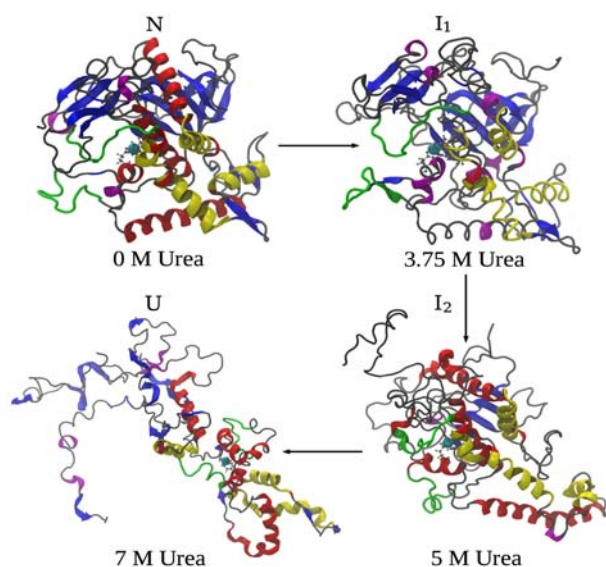

Figure 6.   Structural models of BoNT/A LC from denaturation experiments *in silico*. The α-exocite and β-exocite are shown in yellow and green colors, respectively, and the active site is displayed using the ball-and-stick representation (Zn-ion is shown in cyan). In 0 M urea, all the secondary structure elements are clearly visible and the tertiary structure is intact. In 3.8 M urea solution, BoNT/A LC loses most of its α-helices which convert into random coil, while the β-sheets remain intact and the tertiary structure is preserved. In 5 M urea solution, BoNT/A LC molecule regains α-helicity, yet, loses some β-sheets, and the tertiary structure changes significantly. In 7 M urea solution, BoNT/A LC unfolds completely and loses almost all its tertiary structure elements, while retaining only residual secondary structure content (α-helices).

A stable three-dimensional tertiary structure is considered to be a prerequisite for the biological function of proteins. Paradoxically, there are many examples of proteins that function as MGs or as intrinsically-disordered structures (Uversky, 2002; Vamvaca et al., 2004). Our own results demonstrate that the emergence and thermodynamic stability of these conformational states can be explained by the high structural heterogeneity of their native fold coupled with their intrinsic flexibility (Kukreja & Singh, 2005). In case of BoNT/A, our experiments have established the existence of two stable intermediate conformations (I_1 and I_2) populated in the course of denaturation of BoNT/A LC in aqueous urea solution. This unique dynamic behavior might explain, at least in part, the existence of the active MG state and optimally active PRIME state.

We consider two alternative hypotheses to explain our experimental observations regarding the tendency of BoNT/A LC to self-aggregate, namely that the aggregation takes place by self-association of the protein molecules (1) in the denatured state (U) or (2) in the intermediate state (I_1 and/or I_2). In the first scenario, hydrophobic residues in BoNT/A molecules would be exposed to solvent. This seems unlikely in 3.75 M urea as BoNT/A LC retains most of the secondary structure as detected by FTIR. However, the increase in the amount of random coil and turns ($\sim$59%, Table 1) may lead to more urea molecules gaining access to the interior of the protein. On the other hand, if a protein aggregates under conditions that are intermediate, i.e. interpolate between conditions that favor the native (folded) state and the denatured states, which is the second scenario, then the aggregating species would be in the intermediate conformation (Young, Dill, & Fink, 1993). In general, aggregation kinetics is slow because of a limited access to aggregation – competent conformational states, and it is only over a long period of time that urea might gain access to the protein interior. This would expose hydrophobic residues to solvent, which would then lead to aggregation. Our results indicate that, because BoNT/A molecule is inherently flexible, the aggregation – competent state is easily populated at the intermediate values of urea concentration through losing its α-helicity (intermediate state I_2), which speeds up the aggregation kinetics. This rules out the first scenario as a plausible mechanism for the self-aggregation of BoNT/A in solution.

In case of BoNT/A LC, decreased solubility and self-aggregation in 3.75 M urea solution is not due to the increased accessibility of certain amino acid residues to solvent, but rather because of the urea-induced conformational transitions and emergence of intermediate conformations with exposed hydrophobic residues. This is consistent with the notion that aggregation-competent "seeds" are required to induce aggregation at low to intermediate concentrations of urea (Stigter & Dill, 1993). Increasing urea concentration beyond 3.75 M leads to sequestration of hydrophobic residues from the water environment and partial restoration of the secondary structure (Figures 2 and 6). This conclusion is also supported by the fluorescence intensity data for ANS (8-anilino-1-napthalene sulphonic acid) binding to BoNT/A LC measured at $\lambda = 488$ nm (I_{488}), which shows a decrease in the I_{488} signal for the concentration of urea higher than 3.75 M (see Figure S3 in SM). In 5 M urea solution, combined secondary structure content (α-helices plus β-sheets) is $\sim$59.3% compared with $\sim$66.5% for the native state (FTIR data, Table 1) suggesting a virtual recovery of the protein secondary structure (Figure 2 (A)). This implies that state I_2 is characterized by a substantially-refolded, yet, non-native structure. At higher urea concentrations (above 5 M), most of the protein molecule is denatured, and a further increase in the concentration of denaturing agent leads to spatial separation of protein molecules in solution and weakening of their tendency to aggregate. As a result, protein aggregates formed in 3.75 M urea solution re-dissolve in 5 M urea solution.

Our results from theoretical modeling are in excellent agreement with our experimental findings regarding the unique denaturation mechanism observed for the BoNT/A endopeptidase. Using MD simulations, we have resolved the structural underpinnings which characterize the intermediate states. In addition, we have verified the experimentally-observed helix-to-coil transition in 3.75 M urea solution and have confirmed the stability of α-helices in 3.75 and 5 M urea solution (Figure 6). Our simulation results also indicate that in aqueous urea, α-helices are less stable than β-sheets (especially, in the middle range of urea concentrations). Indeed, in 3.75 M urea solution, the BoNT/A endopeptidase structure is dominated by β-sheets, while almost all α-helical segments have melted forming random coil. Conformational transitions from α-helices to β-sheets are considered to be a hallmark of protein aggregation (Daggett & Levitt, 1992; Fabiana et al., 2009; Monera, Kay, & Hodges, 1994; Vijaykumar, Vishveshwara, Ravishanker, & Beveridge, 1993). We think that this might be the mechanism driving protein aggregation in 3.75 M urea solution. In 5 M urea, the BoNT/A LC molecule regains its α-helical content. This is likely to be caused by the sequestration of amino acid residues exposed to water thus rendering the BoNT/A LC aggregates unstable in the more concentrated solution of urea. In 7 M urea, BoNT/A LC undergoes an almost complete denaturation and only some trace amounts of the secondary structure remain (Figure 6).

An interesting question is why BoNT/A LC is capable of renaturation when incubated in 7 M urea solution but not when incubated in 5 M urea solution? This is evident, e.g. from partial restoration of the enzyme

activity of BoNT/A LC exposed to 7 M urea (Figure 5). Water diffusion slows down significantly in the presence of urea (Bennion & Daggett, 2003). The residence time, i.e. the time during which a urea molecule is in contact with the BoNT/A endopeptidase, which is longer for urea molecules than for water molecules, could be affected to a different extent, due to the different flexibility of the polypeptide chain in the intermediate states I_1 (3.75 M urea) and the uniquely refolded conformation of I_2 (5 M urea), and in the fully denatured state (7 M urea). Also, it is known that urea molecules mediate formation of hydrogen bonds (Rossky, 2008). Hence, urea molecules bound to protein in the intermediate state I_2 might not be easily released even upon dilution, which, in turn, might prevent the BoNT/A molecule from restoring its functional state. Indeed, our renaturation assays performed using urea dilution and dialysis method showed that BoNT/A LC once denatured in urea solution does not regain its native conformation, i.e. the protein partially renatures forming the intermediate state (I_1) but the full renaturation does not occur.

Another interesting question is why BoNT/A LC shows full enzymatic activity with the full-length substrate SNAP-25 for all values of urea concentrations, except for 5 M urea, for which only partial recovery of activity (~55%) was, detected (Figure 5)? This is despite the fact that only partial renaturation from the fully unfolded state (U) in 7 M urea was observed (Figure 2(A)). Interestingly, we found that in the presence of SNAPtide, the level of enzymatic activity upon denaturation in 3.75 M urea is the same as in 7 M urea. Our results also indicate that the biological activity does not correlate well with the secondary or tertiary structure content. To explain this result, we profiled atomic fluctuations for each amino acid residue forming BoNT/A LC. The curves of root mean square deviations (RMSD values) obtained for 0, 3.75, 5, and 7 M urea solution are compared in Figure S4 in SM. We see that amino acid residues in the α-exosite and in the catalytic site, but not in the β-exosite, are characterized by the smallest RMSD values. These determinants seem to form the structural subsystem – α exosite plus the catalytic site, which remains protected even at high concentration of urea. Hence, our results imply that in BoNT/A LC molecule, there is a structural buildup involving the active site which helps preserve the structural basis of its function. Also, the results imply that the β-exosite, characterized by large RMSD values, plays a minor role in BoNT/A being enzymatically active compared with the α-exosite. These findings also agree with the results of recent experiments, wherein, small (large) conformational changes were observed in the α-exosite (β-exosite) (Breidenbach & Brunger, 2004).

In conclusion, protein folding remains a challenging problem notwithstanding the substantial advances in protein crystallography, Nuclear Magnetic Resonance, various folding–unfolding techniques, and theoretical modeling (England & Haran, 2011; Fersht & Daggett, 2002; Scheraga, Khalili, & Liwo, 2007). How a protein folds into a well-defined and biologically-active three-dimensional structure from a linear sequence of amino acids is a fascinating field of research. In the context of enzymes, the main challenge is to link the folded state of a protein with its functional activity. In this regard, the BoNT/A system offers a new paradigm to revisit the problem of protein folding in relation to functional activity. Here, we showed that BoNT/A LC undergoes the unique unfolding transition through formation of stable intermediate states, which display a remarkable correlation between their structure and function. The unique folding mechanism of BoNT endopeptidase and its unusual structural heterogeneity may have not only functional implications for its biological activity, but also far reaching consequences for its stability. The dynamically flexible structure of BoNT/A LC may contribute to the functional longevity of BoNT/A intracellularly. Hence, BoNT/A LC presents a unique example to explore the interplay between the protein stability and dynamics. In a sense, structural flexibility afforded by protein folding might be an evolved trait for the survival of proteins intracellularly and for performing their biological actions.

Supplementary material

The supplementary material for this paper is available online at http://dx.doi.10.1080/07391102.2013.791878.

Acknowledgments

Abbreviations

BoNT	botulinum neurotoxin
MG	molten globule
SNARE	soluble NSF attachement protein receptor
MD	Molecular Dynamics
CD	circular dichroism
CHARMM22	chemistry at Harvard molecular mechanics
NAMD	not (just) another molecular dynamic program
VMD	Visual Molecular Dynamic
FTIR	Fourier Transform Infrared Spectroscopy
NMR	Nuclear Magnetic Resonance

References

Adler, M., Keller, J. E., Sheridan, R. E., & Deshpande, S. S. (2001). Persistence of botulinum neurotoxin A demonstrated by sequential administration of serotypes A and E in rat EDL muscle. *Toxicon, 39*, 233–243.

Bennion, B. J., & Daggett, V. (2003). The molecular basis for the chemical denaturation of proteins by urea. *Proceedings of the National academy of Sciences of the USA, 100*, 5142–5147.

Boldt, G. E., Kennedy, J. P., Hixon, M. S., McAllister, L. A., Barbieri, J. T., Tzipori, S., & Janda, K. D. (2006). Synthesis, characterization and development of a high-throughput methodology for the discovery of botulinum neurotoxin a inhibitors. *Journal of Combinatorial Chemistry, 8*, 513–521.

Breidenbach, M. A., & Brunger, A. T. (2004). Substrate recognition strategy for botulinum neurotoxin serotype A. *Nature, 432*, 925–929.

Burnett, J. C., Schmidt, J. J., McGrath, C. F., Nguyen, T. L., Hermone, A. R., Panchal, R. G., … Baveri, S. (2005). Conformational sampling of the botulinum neurotoxin serotype A light chain: Implication for inhibitor binding. *Bioorganic & Medicinal Chemistry, 13*, 333–341.

Cai, S., & Singh, B. R. (2001a). Role of the disulfide cleavage induced molten globule state of type A botulinum neurotoxin in the endopeptidase activity. *Biochemistry, 40*, 15327–15333.

Cai, S., & Singh, B. R. (2001b). A correlation between differential structural features and the degree of endopeptidase activity of type A botulinum neurotoxin in aqueous solution. *Biochemistry, 40*, 4693–4702.

Daggett, V., & Levitt, M. (1992). A model of the molten globule state from molecular dynamics simulations. *Proceedings of the National academy of Sciences of the USA, 89*, 5142–5146.

Dolly, J. O., & Aoki, K. R. (2006). The structure and mode of action of different botulinum toxins. *European Journal of Neurology, 13*, 1–9.

England, J. L., & Haran, G. (2011). Role of solvation effects in protein denaturation: From thermodynamics to single molecule and back. *Annual Review of Physical Chemistry, 62*, 257–277.

Fabiana, E., Stadler, A. M., Madern, D., Koza, M. M., Tehel, M., Hirai, M., & Zaccai, G. (2009). Dynamics of apomyoglobin in the α-to-β transition and of partially unfolded aggregated protein. *European Biophysics Journal, 38*, 237–244.

Fersht, A. R., & Daggett, V. (2002). Protein folding and unfolding at atomic resolution. *Cell, 108*, 1–20.

Humphrey, W., Dalke, A., & Schulten, K. (1996). VMD-visual molecular dynamics. *Journal of Molecular Graphics, 14*, 33–38.

Jorgensen, W. L., Chandrasekhar, J., Madura, J. D., Impey, R. W., & Klein, M. L. (1983). Comparison of simple potential functions for simulating liquid water. *Journal of Chemical Physics, 79*, 926–935.

Katona, P. (2012). Botulinum toxin: Therapeutic agent to cosmetic enhancement to lethal biothreat. *Anaerobe, 18*, 240–243.

Kukreja, R. V., Sharma, S. K., & Singh, B. R. (2010). Molecular basis of activation of endopeptidase activity of botulinum neurotoxin type E. *Biochemistry, 49*, 2510–2519.

Kukreja, R., & Singh, B. R. (2005). Biologically active novel conformational state of botulinum, the most poisonous poison. *Journal of Biological Chemistry, 280*, 39346–39352.

Li, L., & Singh, B. R. (2000). Spectroscopic analysis of pH-induced changes in the molecular features of type A botulinum neurotoxin light chain. *Biochemistry, 39*, 6466–6474.

Lopez, G., Bañares-Hidalgo, A., & Estrada, P. (2011). Xylanase II from *Trichoderma reesei* QM 9414: Conformational and catalytic stability to chaotropes, trifluoroethanol, and pH changes. *Journal of Industrial Microbiology and Biotechnology, 38*, 113–125.

MacKerell, A. D., Bashford, D., Bellott, M., Dunbrack, R. L., Evanseckl, D., Field, M. J., … Karplus, M. (1998). All-atom empirical potential for molecular modeling and dynamics studies of proteins. *Journal of Physical Chemistry B, 102*, 3586–3616.

Monera, O. D., Kay, C. M., & Hodges, R. S. (1994). Protein denaturation with guanidine hydrochloride or urea provides a different estimate of stability depending on the contributions of electrostatic interactions. *Protein Science, 3*, 1984–1991.

Montecucco, C., & Schiavo, G. (1993). Tetanus and botulinum neurotoxins: A new group of zinc proteases. *Trends in Biochemical Sciences, 18*, 324–327.

Phillips, J. C., Braun, R., Wang, W., Gumbart, J., Tajkhorshid, E., Villa, E., … Schulten, K. (2005). Scalable molecular dynamics with NAMD. *Journal of Computational Chemistry, 25*, 1781–1802.

Pickett, A., & Perrow, K. (2011). Towards new uses of botulinum toxins as a novel therapeutic tool. *Toxins (Basel), 3*, 63–81.

Ptitsyn, O. B., Pain, R. H., Semisotnov, G. V., Zerovnik, E., & Razgulyaev, O. I. (1990). Evidence for a molten globule state as a general intermediate in protein folding. *FEBS Letters, 262*, 20–24.

Rossky, P. J. (2008). Protein denaturation by urea: Slash and bond. *Proceedings of the National academy of Sciences of the USA, 105*, 16825–16826.

Scheraga, H. A., Khalili, M., & Liwo, A. (2007). Protein-folding dynamics: Overview of molecular simulation techniques. *Annual Review of Physical Chemistry, 58*, 57–83.

Segelke, B., Knapp, M., Kadkhodaya, S., Balhorn, R., & Ruoo, B. (2004). Crystal structure of *Clostridium botulinum* neurotoxin protease in a product-bound state: Evidence for noncanonical zinc protease activity. *Proceedings of the National academy of Sciences of the USA, 101*, 6888–6893.

Singh, B. R. (2009). Special editorial – "Menace or the ultimate medicine – a case for botulinum neuromedicine". *The Botulinum Journal, 1*, 257–260.

Stephan, S., & Wang, T. D. (2011). Botulinum toxin: Clinical techniques, applications, and complications. *Facial Plastic Surgery, 27*, 529–539.

Stigter, D., & Dill, K. A. (1993). Theory for protein solubilities. *Fluid Phase Equilibria, 82*, 237–249.

Tonello, F., Morante, S., Rossetto, O., Schiavo, G., & Montecucco, C. (1996). Tetanus and botulism neurotoxins: A novel group of zinc-endopeptidases. *Advances in Experimental Medicine and Biology, 389*, 251–260.

Tsou, C. (1995). Inactivation precedes overall molecular conformation changes during enzyme denaturation. *Biochimica et Biophysica Acta, 1253*, 151–162.

Uversky, V. N. (2002). What does it mean to be natively unfolded? *European Journal of Biochemistry, 269*, 2–12.

Uversky, V. N., Kutyshenko, V. P., Protasova, N. Yu, Rogov, V. V., Vassilenko, K. S., & Gudkov, A. T. (1996). Circularly permuted dihydrofolate reductase possesses all the properties of the molten globule state, but can resume functional tertiary structure by interaction with its ligands. *Protein Science, 5*, 1844–1851.

Vamvaca, K., Vogeli, B., Kast, P., Pervushin, K., & Hilvert, D. (2004). An enzymatic molten globule: Efficient coupling of folding and catalysis. *Proceedings of the National academy of Sciences of the USA, 101*, 12860–12864.

Vijaykumar, S., Vishveshwara, S., Ravishanker, G., & Beveridge, D. L. (1993). Differential stability of β-sheets and α-helices in β-lactamase: A high temperature molecular dynamics study of unfolding intermediates. *Biophysical Journal, 65*, 2304–2312.

Young, L. R. D., Dill, K. A., & Fink, A. L. (1993). Aggregation and denaturation of apomyoglobin in aqueous urea solution. *Biochemistry, 32*, 3877–3886.